JACS
JOURNAL OF THE AMERICAN CHEMICAL SOCIETY
Article
Cite This: J. Am. Chem. Soc. 2018, 140, 8340−8349
pubs.acs.org/JACS

In Situ Atomic-Level Tracking of Heterogeneous Nucleation in Nanocrystal Growth with an Isocyanide Molecular Probe

Yiren Wu and Dong Qin*

School of Materials Science and Engineering, Georgia Institute of Technology, Atlanta, Georgia 30332, United States

Supporting Information

ABSTRACT: We report the use of 2,6-dimethylphenyl isocyanide (2,6-DMPI) as a spectroscopic probe to study the heterogeneous nucleation and deposition of Pd on Ag nanocubes under different conditions by surface-enhanced Raman scattering. As a major advantage, the spectroscopic analysis can be performed in situ and in real time with the nanoparticles still suspended in the reaction solution. The success of this method relies on the distinctive stretching frequencies (ν_{NC}) of the isocyanide group in 2,6-DMPI when it binds to Ag and Pd atoms through σ donation and π-back-donation, respectively. Significantly, we discovered that ν_{NC} was sensitive to the arrangement of Pd adatoms on the Ag surface. For example, when the isocyanide group bound to one, two, and three Pd atoms, we would observe the atop, bridge, and hollow configurations, respectively, at different ν_{NC} frequencies. As such, the ν_{NC} band could serve as a characteristic reporter for the Pd adatoms being deposited onto different types of facets on Ag nanocubes with atomic-level sensitivity. When 2,6-DMPI molecules were introduced into the reaction solution, we further demonstrated in situ tracking of heterogeneous nucleation and early stage deposition of Pd on Ag nanocubes by monitoring the evolution of ν_{NC} bands for both Ag and Pd surface atoms as a function of reaction time. This in situ technique opens up the opportunity to investigate the roles played by reaction temperature and the type of Pd(II) precursor in influencing the heterogeneous nucleation and growth of bimetallic nanocrystals. The sensitivity of isocyanide group to Pd atoms helps elucidate some of the details on the reduction, deposition, and diffusion processes involved in heterogeneous nucleation.

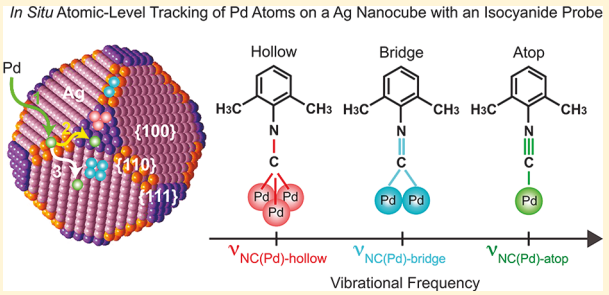

1. INTRODUCTION

The development of in situ methods for characterizing metal-molecule interactions in a liquid phase or other ambient environments plays an essential role in advancing interfacial science for applications in heterogeneous catalysis and electrocatalysis.[1−6] As an alternative to the techniques based on electron beam, surface-enhanced Raman scattering (SERS) has emerged as a powerful tool for probing molecular vibrations in proximity to the surface of plasmonically active metals such as Ag, Au, or Cu, with excellent sensitivity in detecting molecular structure and bonding at the interface.[7−12] Thiol-based molecules have been most commonly used as SERS probes, with notable examples including 1,4-benzenedithiol and 4-nitrothiophenol. Although the vibrational modes associated with their benzene ring are strong enough to allow for ultrasensitive detection of these molecules upon adsorption onto the surface of Ag or Au nanocrystals,[13−16] these vibrational modes show essentially no dependence on the metal surface, making them invalid for the identification of different metals.

Recent studies suggest that isocyanide compounds could serve as metal-sensitive SERS probes because the binding of the isocyanide group (−NC) to a transition metal is similar to that of carbon monoxide (CO) due to their isoelectronic structure.[17,18] To this end, a number of research groups reported distinctive stretching frequencies (ν_{NC}) for the NC bond when the −NC group binds to different types of metals in the context of nanoparticles, powders, and crystal substrates. For example, Shin et al. reported that the ν_{NC} band was positioned at 2175 and 2107 cm^{-1}, respectively, when 2,6-dimethylphenyl isocyanide (2,6-DMPI) was introduced as a SERS probe to coordinate with the Ag and Pd (on Ag−Pd alloy nanoparticles) atoms.[19] Sanchez-Cortes et al. studied the adsorption of 1,4-phenylene diisocyanide (1,4-PDI) on Ag and Au nanoparticles, and they argued that the two different SERS peaks located at 2182 and 2125 cm^{-1} could be assigned to bounded and unbounded −NC groups on Ag, respectively.[20] Zou et al. reported the SERS study of 1,4-PDI adsorbed on Au, Pt, Rh, and Pd electrodes.[21] They revealed that the frequency of ν_{NC} was strongly dependent on the metal to which the isocyanide group bound. Ikeda et al. investigated the adsorption of 4-chlorophenyl isocyanide (4-CPI) on a single-crystal Pt surface using gap-mode SERS.[22] They also observed the formation of Pd islands on the surface of a Au(111) substrate by employing 4-CPI as a SERS probe.[23] Taken together, it has been well-established that the lone-pair electrons associated with the carbon atom in the −NC group

Received: May 8, 2018
Published: June 13, 2018

DOI: 10.1021/jacs.8b04824
J. Am. Chem. Soc. 2018, 140, 8340−8349

could bind to the surface of Ag or Au via σ donation and to that of Pt or Pd via π-back-donation, leading to blue and red shifts, respectively, for ν_{NC}.

Most recently, we proposed that the isocyanide-based SERS probe could serve as a distinctive reporter for investigating the heterogeneous nucleation and early stage deposition of the transition metal such as Pt on the plasmonic Ag or Au nanocrystals by monitoring the change to the frequency of ν_{NC} with in situ SERS. As the first proof-of-concept demonstration, we reported the use of 2,6-DMPI as a SERS probe for watching the overgrowth of Pt on Ag nanocubes in the original growth solution.[24] By monitoring the stretching frequencies and the peak intensities of ν_{NC} in real time, we demonstrated that in situ SERS had the sensitivity to detect as few as 27 Pt atoms being deposited onto each edge of a 39 nm Ag nanocube. Despite the remarkable detection sensitivity, we only observed one peak for ν_{NC} when 2,6-DMPI bound to Pt atoms in the atop configuration, making it impossible to further characterize the atomic arrangement of Pt atoms during the heterogeneous nucleation and early stage deposition events.

According to the literature, the binding of CO to Pd atoms could take the atop, bridge, and hollow configurations.[25−27] As such, we propose that 2,6-DMPI can bind to Pd atoms in these three different configurations, making it feasible to characterize the arrangement of Pd atoms being deposited onto different types of facets of Ag nanocubes by monitoring the vibrational frequency of ν_{NC} (Figure 1). Specifically, the 2,6-DMPI probe

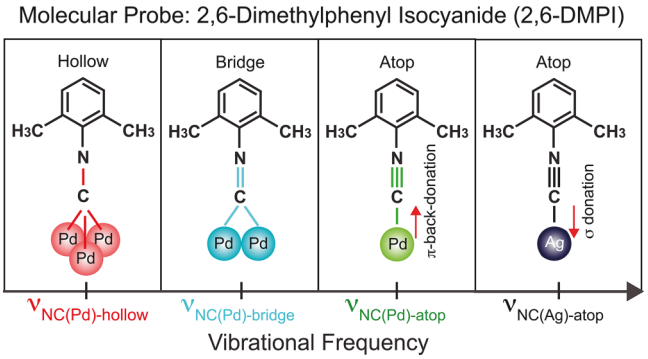

Figure 1. Schematic illustration showing the difference in stretching frequency for the NC bond, ν_{NC}, when 2,6-DMPI binds to Ag in the atop configuration and to the Pd atoms in the atop, bridge, and hollow configurations, respectively.

should bind to Ag and Pd via σ donation and π-back-donation, respectively, resulting in a blue shift for $\nu_{NC(Ag)\text{-atop}}$ and a red shift for $\nu_{NC(Pd)\text{-atop}}$ accordingly.[19] Similar to the case of CO, we believe that −NC can also bind to one, two, and three adjacent Pd atoms for the generation of atop, bridge, and hollow configurations, respectively.[27] Because the bond between the N and C atoms will be gradually weakened as −NC shares electrons with one, two, and three Pd atoms, the vibrational frequencies of $\nu_{NC(Pd)\text{-atop}}$, $\nu_{NC(Pd)\text{-bridge}}$, and $\nu_{NC(Pd)\text{-hollow}}$ should be further shifted to the red.

In this article, we report in situ atomic-level tracking of the heterogeneous nucleation of Pd on Ag nanocubes by using the 2,6-DMPI as a sensitive molecular probe. We demonstrate that the ν_{NC} band of 2,6-DMPI can serve as a distinctive reporter for the Pd adatoms being deposited on the surface of Ag nanocubes with atomic-level sensitivity. In the case of ex situ measurement, we follow a standard protocol to synthesize Ag−Pd nanocubes by adding Na_2PdCl_4 into the aqueous suspension of Ag nanocubes in the presence of ascorbic acid (H_2Asc, a reducing agent) and poly(vinylpyrrolidone) (PVP, a colloidal stabilizer) under ambient condition. After collecting the solid products, we functionalize the nanoparticles with 2,6-DMPI molecules for ex situ SERS characterization. We are able to detect the $\nu_{NC(Pd)\text{-atop}}$, $\nu_{NC(Pd)\text{-bridge}}$, and $\nu_{NC(Pd)\text{-hollow}}$ bands in the SERS spectra, confirming that 2,6-DMPI can indeed serve as a probe to distinguish the Pd adatoms in terms of arrangement. Because the ex situ method often requires centrifugation and washing, during which the Pd adatoms can migrate from the original sites of deposition prior to SERS measurements, we also develop an in situ approach. In this case, we directly introduce 2,6-DMPI into the standard reaction solution and then sample aliquots at different time points for SERS measurement. We confirm that the presence of 2,6-DMPI in the reaction solution does not alter the reduction of the precursor, neither the deposition pathway of Pd on Ag nanocubes. We further demonstrate the capability of this in situ method for atomic-level tracking of Pd atoms being deposited on the Ag nanocubes by following the ν_{NC} bands for both Ag and Pd atoms as a function of reaction time. The different binding configurations of −NC to Pd atoms also offer an opportunity to investigate the roles played by reaction temperature and the type of Pd(II) precursor in affecting the reduction, deposition, and surface diffusion involved in heterogeneous nucleation.

2. EXPERIMENTAL SECTION

2.1. Chemicals and Materials. Poly(vinylpyrrolidone) (PVP) with an average molecular weight of 29 000 (PVP-29k) or 55 000 (PVP-55k), L-ascorbic acid (H_2Asc, ≥ 98%), 2,6-dimethylphenyl isocyanide, (2,6-DMPI, ≥ 98%), ethanol (CH_3CH_2OH, 200 proof), sodium tetrachloropalladate(II) (Na_2PdCl_4, ≥ 99.99% trace metal basis), silver trifluoroacetate (CF_3COOAg, ≥ 99.99% trace metal basis), sodium hydrosulfide hydrate ($NaHS{\cdot}xH_2O$), aqueous hydrochloric acid (HCl, 37%), hydrogen peroxide (H_2O_2, 30 wt % in H_2O), and iron(III) nitrate nonahydrate ($Fe(NO_3)_3{\cdot}9H_2O$, ≥ 98%) were all purchased from Sigma-Aldrich. Ethylene glycol ($HOCH_2CH_2OH$, EG) was ordered from J.T. Baker. Acetone (HPLC grade, 99.5+%) and sodium tetrabromopalladate(II) (Na_2PdBr_4, 99.95% trace metal basis, Pd 22.0% min) were obtained from Alfa Aesar. All the chemicals were used as-received. The deionized (DI) water had a resistivity of 18.2 MΩ·cm at room temperature.

2.2. Synthesis of Silver Nanocubes. We followed a published protocol to synthesize the Ag nanocubes.[28] The products were washed with acetone and DI water three times and then dispersed in DI water for further use. The suspension of Ag nanocubes had a final concentration of 6.56×10^{12} particles/mL.

2.3. Synthesis of Ag−Pd Nanocubes. In a typical synthesis, 2 mL of 1 mM PVP-29k aqueous solution was placed in a 23 mL vial, followed by the introduction of 0.5 mL of 100 mM aqueous H_2Asc, 0.5 mL of DI water, and 25 μL of the aqueous suspension of Ag nanocubes (1.64×10^{11} particles) at room temperature under magnetic stirring. Different volumes of aqueous Na_2PdCl_4 (0.2 mM) were then injected into the vial using a pipet. After 20 min, the solid products were collected by centrifugation at 6000 rpm for 10 min and redispersed in DI water for further use.

2.4. Raman Measurements. The Raman spectra were recorded using a Renishaw inVia Raman Spectrometer integrated with a Leica microscope. The excitation wavelength was 532 nm, and the scattered light was dispersed using a holographic notch filter with a grating of 2400 lines/mm. For all the time-dependent SERS spectra, they were collected using either *static* or *extended* mode. In the *static* mode, we recorded a Raman spectrum in the range of 1445.83−2495.29 cm^{-1} by setting the center position at 2000 cm^{-1} almost instantaneously,

DOI: 10.1021/jacs.8b04824
J. Am. Chem. Soc. 2018, 140, 8340−8349

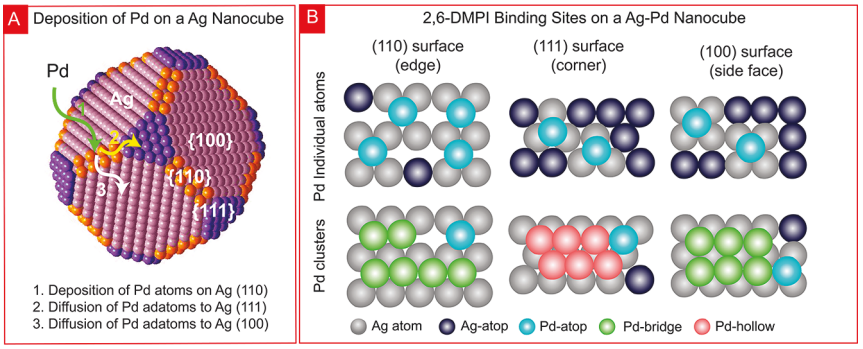

Figure 2. (A) Schematic diagram of a proposed pathway for the deposition of Pd atoms on a Ag nanocube. (B) Schematic illustrations showing the different binding sites and configurations for Pd atoms on the surface of a Ag nanocube.

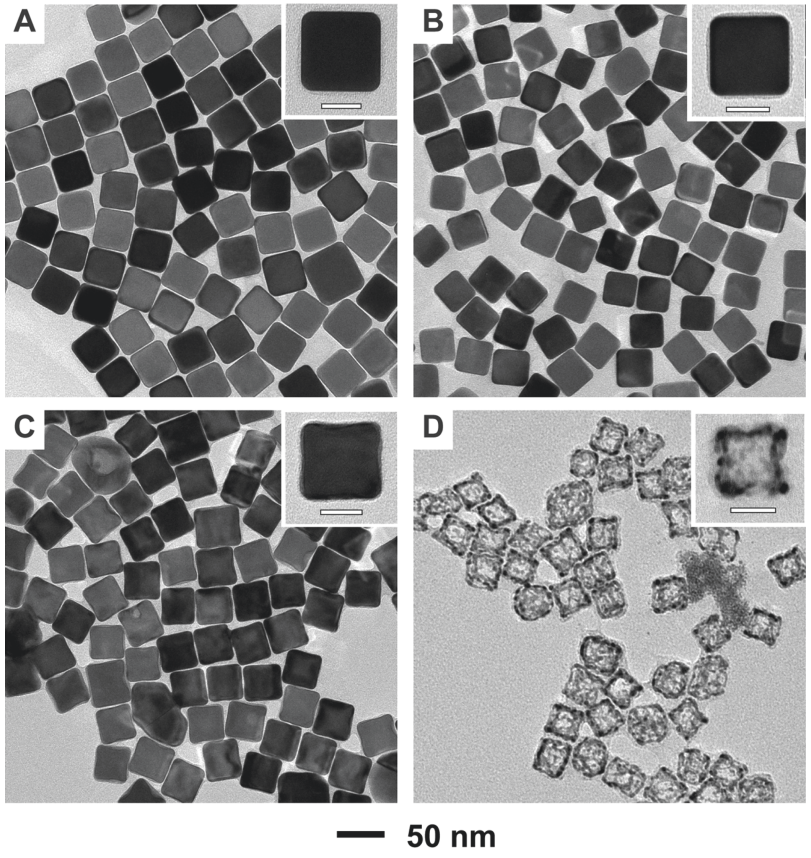

Figure 3. TEM images of (A) Ag nanocubes, (B, C) Ag−Pd nanocubes prepared by reacting 40 nm Ag nanocubes with 50 and 600 μL of aqueous Na_2PdCl_4, respectively, in the presence of H_2Asc and PVP, and (D) the resultant Ag−Pd nanoframes after the removal of Ag cores from the Ag−Pd nanocubes in (C) using an etchant based on $Fe(NO_3)_3/HNO_3$. The scale bar in the inset is 20 nm.

within a period as short as 1 s. We typically used a collection time of 10 s to improve the signal-to-noise ratio by averaging multiple spectra. In the *extended* mode, it took about 90 s for the spectrometer to scan across the spectral region from 500 to 2500 cm^{-1} when a collection time of 10 s was used.

2.5. Ex Situ SERS Measurements. The as-prepared particles were dispersed in 1 mL of ethanol containing 0.01 mM 2,6-DMPI and incubated at room temperature for 60 min. Next, the 2,6-DMPI-functionalized nanocubes were collected by centrifugation and washed with DI water twice and redispersed in 200 μL of DI water, with a final concentration of 1.3×10^{10} particles/mL. We fabricated the sample cell by punching a hole, which could hold 25 μL of liquid, in the surface of a polydimethylsiloxane (PDMS) block and then having it mounted on a piece of glass slide. Upon the introduction of liquid sample, the cell was carefully covered with a glass coverslip of 0.17 mm in thickness to avoid solvent evaporation. The top surface of the coverslip could also work as a reference point, from which the focal plane was defined at 200 μm into the sample. We collected the SERS spectra in the *extended* mode, with a 5× objective lens, a laser power of 50 mW, and a collection time of 10 s.

2.6. In Situ SERS Measurements in the Reaction Solution. In a typical study, 2 mL of 1 mM PVP-29k aqueous solution was introduced into a 23 mL vial, followed by the addition of 0.5 mL of 100 mM aqueous H_2Asc and 0.5 mL of 0.01 mM 2,6-DMPI in ethanol at room temperature (21 °C) under magnetic stirring (650 rpm). For the temperature dependent experiments, the reaction container was immersed in an ice bath (0 °C) or oil bath (40 °C) for 30 min. Initially, an aliquot of 25 μL was withdrawn from the mixture and a solution-phase Raman spectrum was recorded before 25 μL of an aqueous suspension of Ag nanocubes (1.64×10^{11} particles in total) was added. After 10 min, an aliquot of 25 μL was withdrawn from the reaction solution and a SERS spectrum was recorded.

DOI: 10.1021/jacs.8b04824
J. Am. Chem. Soc. 2018, 140, 8340−8349

Finally, 50 μL of 0.2 mM aqueous Na_2PdCl_4 (or 50 μL of 0.2 mM aqueous Na_2PdBr_4) was introduced using a pipet. At different time points of reaction, an aliquot of 25 μL was quickly withdrawn from the reaction solution and its SERS spectrum was recorded in the *extended* mode, with a 5× objective lens, a laser power of 50 mW, and a collection time of 10 s. After 60 min, the remaining particles were collected by centrifugation and washed with DI water three times prior to TEM characterization.

We also recorded in situ SERS spectra of the reaction mixture in the *static* mode. In this case, an aliquot of 25 μL was withdrawn from the same reaction system at a specific time point and subjected to SERS measurement with a 5× objective lens, a laser power of 50 mW, and a collection time of 1 or 10 s.

2.7. Instrumentation and Characterization. We used a centrifuge (Eppendorf 5430) for the collection and washing of all solid products. A Cary 50 spectrometer (Agilent Technologies, Santa Clara, CA) was used to record the UV−vis spectra. The quantitative measurement of Ag and Pd contents was conducted using an inductively coupled plasma mass spectrometer (ICP-MS, NexION 300Q, PerkinElmer, Waltham, MA). Transmission electron microscopy (TEM) images were taken using a Hitachi HT7700 microscope (Hitachi, Japan) operated at 120 kV. The Raman and SERS spectra were recorded using a Renishaw inVia Raman Spectrometer (Wotton-under-Edge, U.K.) integrated with a Leica microscope (Wetzlar, Germany).

3. RESULTS AND DISCUSSION

3.1. Analysis of the SERS Detection Mechanism. Figure 2 shows how SERS can be used for in situ, atomic-level tracking of the heterogeneous nucleation of Pd on a Ag nanocube with the aid of 2,6-DMPI. As reported in literature[29−32] and illustrated in Figure 2A, the Pd atoms should be preferentially deposited on the edges, terminated in {110} facets, of a Ag nanocube, followed by the diffusion of Pd adatoms to corners and side faces that correspond to {111} and {100} facets, respectively. Our calculations based on the finite element method (FEM) indicate that the SERS hot spots of a 40 nm Ag nanocube are predominantly located on the edges.[24] Our results suggest that the electromagnetic field can also be enhanced at sites in close proximity to the edges, including those regions on the corners and side faces. When 2,6-DMPI binds to the surface atoms on a Ag−Pd nanocube, Figure 2B illustrates two scenarios. In the first scenario (top panel), which corresponds to the early stage of a synthesis, Pd is deposited as individual adatoms on the outermost surface of a Ag nanocube. As a result, 2,6-DMPI binds to both the Pd adatoms and the remaining Ag atoms in the atop configuration only. In the second scenario (bottom panel), as the deposition of Pd progresses toward a monolayer to generate Pd clusters on the Ag surface, 2,6-DMPI can bind to the Pd adatoms in the atop, bridge, and hollow configurations, respectively. According to the atomic arrangement, the Pd adatoms on the {111} facets (the corners) can give rise to atop and hollow configurations while the {110} facets (edges) and {100} facts (side faces) only allow for atop and bridge configurations. Taken together, we hypothesize that 2,6-DMPI can serve as a unique probe to characterize the arrangements of Pd adatoms being deposited onto different types of facets on Ag nanocubes by monitoring the peak intensities of the $\nu_{NC(Pd)\text{-}atop}$, $\nu_{NC(Pd)\text{-}bridge}$, and $\nu_{NC(Pd)\text{-}hollow}$ bands.

3.2. Synthesis of Ag−Pd Nanocubes. After the preparation of Ag nanocubes with an average edge length of 40.3 ± 1.6 nm (Figure 3A),[28] we dispersed them in an aqueous solution containing H_2Asc and PVP, followed by the injection of aqueous Na_2PdCl_4 under ambient condition. Figure 3, B and C, shows TEM images of the as-obtained Ag−Pd nanocubes prepared with the introduction of 50 and 600 μL of Na_2PdCl_4 solution, respectively. In both cases, we noticed that the cubic shape of the nanocubes was well retained. To resolve the sites of deposition for Pd on the surface of Ag nanocubes, we used an aqueous mixture of $Fe(NO_3)_3$ and HNO_3 to remove the Ag core while retaining the Pd. We were unable to collect any solid by centrifugation for the sample prepared with 50 μL of aqueous Na_2PdCl_4. When the amount of Na_2PdCl_4 solution was increased to 600 μL, however, we obtained nanoframes, as shown by the TEM image in Figure 3D. This result suggests that the Pd atoms derived from the reduction of Na_2PdCl_4 by H_2Asc were preferentially deposited on the edges of the Ag nanocubes, together with the diffusion of some Pd adatoms to the corners and side faces. This result is consistent with the deposition mechanism proposed in Figure 2A.

To further confirm the deposition of Pd atoms on the Ag nanocubes, we used ICP-MS to measure Ag and Pd contents in both solid and supernatant before and after the Ag nanocubes had reacted with 50 μL of aqueous Na_2PdCl_4 in the presence of H_2Asc and PVP (Table S1 of the Supporting Information, SI). The ICP-MS data indicated that 46.6% of the added Na_2PdCl_4 was converted to Pd atoms, followed by their deposition onto the Ag nanocubes. If we assumed that these Pd atoms were deposited uniformly on all the edges of the Ag nanocubes with the dimensions defined in Figure S1, we estimated that 1006 Pd atoms would be deposited on each edge. The same back-of-the-envelope calculation suggested that 1189 Pd atoms would be needed for generating one monolayer of Pd adatoms on each edge of a nanocube (see details in Appendices 1−3). On the basis of these results, we decided to focus on the two systems involving 10 and 50 μL of Na_2PdCl_4 solution when designing experiments to monitor the heterogeneous nucleation and deposition of Pd on the Ag nanocubes by SERS. It is worth mentioning that the added Na_2PdCl_4 could be reduced by both H_2Asc via chemical reduction and Ag via galvanic replacement. Because the morphology of the Ag−Pd nanocubes obtained using 50 μL of Na_2PdCl_4 solution was similar to that of the original Ag nanocubes (see Figure 3B), we argue that the reduction of Na_2PdCl_4 should be dominated by H_2Asc rather than by Ag. Otherwise, we expect to observe changes to the morphology.

3.3. Resolving the Arrangement of Pd Adatoms on Ag Nanocubes by Ex Situ SERS. In a typical process, we incubated the as-prepared Ag−Pd nanocubes in an ethanol solution of 0.01 mM 2,6-DMPI for 60 min, followed by the collection of solids through centrifugation. After the particles had been washed with DI water twice, they were redispersed in DI water for SERS measurements. Figure 4 shows the SERS spectra of 2,6-DMPI adsorbed on the Ag−Pd nanocubes prepared with 10 and 50 μL of Na_2PdCl_4 solution. For the case of 10 μL, the SERS spectrum showed two major peaks at 2170 and 2108 cm^{-1}, with their assignment to the NC stretching of the probe molecules binding to Ag ($\nu_{NC(Ag)\text{-}atop}$) and Pd ($\nu_{NC(Pd)\text{-}atop}$), respectively.[19] When compared with the ν_{NC} band at 2123 cm^{-1} for the ordinary Raman spectrum of 2,6-DMPI in the neat state (Figure S2), we noticed that the $\nu_{NC(Ag)\text{-}atop}$ and $\nu_{NC(Pd)\text{-}atop}$ bands were blue- and red-shifted, respectively. The ratio between the peak intensities of the $\nu_{NC(Pd)\text{-}atop}$ and $\nu_{NC(Ag)\text{-}atop}$ bands was 2.79:1. The other well-resolved peaks were associated with different vibrational modes of the benzene ring in 2,6-DMPI (see Table S2 for peak assignments).[19] We also observed some peaks belonging to

DOI: 10.1021/jacs.8b04824
J. Am. Chem. Soc. 2018, 140, 8340−8349

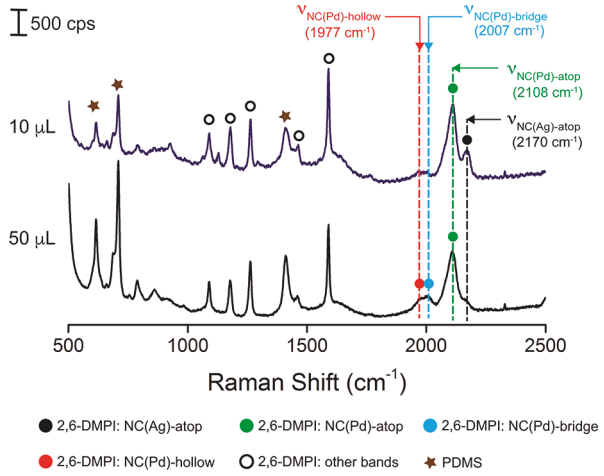

Figure 4. Ex situ SERS spectra recorded from aqueous suspensions of 2,6-DMPI-functionalized samples prepared by reacting 40 nm Ag nanocubes with 10 and 50 μL, respectively, of Na_2PdCl_4 in the presence of H_2Asc and PVP at room temperature.

PDMS (marked by solid stars, see Figure S3 for an ordinary Raman spectrum of PDMS and Table S3 for their peak assignments).[33] Taken together, we hypothesized that the Pd was deposited on the edges of the Ag nanocubes as individual atoms. Likely, some of the Pd adatoms could undergo surface diffusion to the corners and side faces, but remaining as individual atoms. This observation suggests that 2,6-DMIP bound to the surface of the Ag−Pd nanocubes in the pattern illustrated in the top panel of Figure 2B. For the case of 50 μL, the $\nu_{NC(Pd)-atop}$ peak became more dominant while the $\nu_{NC(Ag)-atop}$ band evolved into a shoulder peak. Meanwhile, we observed two weak peaks at 2007 and 1977 cm^{-1}, which could be assigned to $\nu_{NC(Pd)-bridge}$ and $\nu_{NC(Pd)-hollow}$, respectively.[19] This result indicated that, as more Pd was deposited on the Ag nanocubes, the Pd adatoms would start to form clusters on the edges, and subsequently the corners and side faces because of surface diffusion, leading to the binding pattern depicted in bottom panel of Figure 2B.

3.4. Probing the Heterogeneous Nucleation of Pd Atoms on Ag nanocubes by In Situ SERS. One of the challenges in using the ex situ SERS method to monitor the deposition of Pd on Ag nanocubes is that the samples often need to go through several centrifugation steps prior to SERS measurements. In this case, it is possible that the Pd adatoms can migrate from the original sites of deposition during the sample preparation process, making it difficult to capture the original arrangements of Pd adatoms during deposition. One approach to eliminate this ambiguity is to directly introduce 2,6-DMPI into the reaction solution to monitor the Pd atoms being deposited on Ag nanocubes through in situ SERS. In a typical experiment, we prepared a standard aqueous solution containing PVP, H_2Asc, and 2,6-DMPI (in ethanol), followed by the addition of Ag nanocubes and then 50 μL of aqueous Na_2PdCl_4 under magnetic stirring at room temperature (21 °C). Aliquots were sampled from the reaction solution for immediate characterization by SERS.

Figure 5 shows a series of Raman/SERS spectra obtained by withdrawing samples from the reaction solution at different time points and then subjecting to Raman measurements (see details in the Experimental Section). The Raman spectrum recorded from the aqueous solution containing PVP, H_2Asc, and 2,6-DMPI only showed a set of peaks that could be assigned to the vibrational bands of PDMS (marked by solid stars)[33] and ethanol (marked by open stars, see Figure S4 for an ordinary Raman spectrum of ethanol and Table S4 for the peak assignments).[34] In fact, we could use the ethanol peak at 879 cm^{-1} as an internal standard to calibrate the SERS spectra because the position and peak intensity of this band remained essentially the same in the entire course of an experiment. After 10 min post the addition of Ag nanocubes, the peak of $\nu_{NC(Ag)-atop}$ at 2162 cm^{-1} (marked by black dot) appeared on the spectrum, indicating the adsorption of 2,6-DMPI onto the surface of Ag nanocubes. When aqueous Na_2PdCl_4 was introduced, we argued that the reduction of Na_2PdCl_4 by

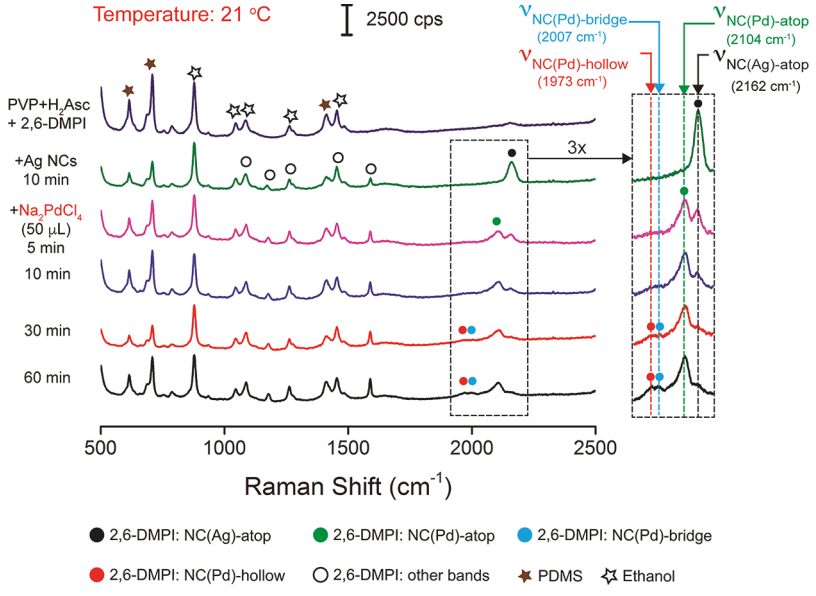

Figure 5. Raman spectrum recorded from an aqueous solution containing 2,6-DMPI (predissolved in ethanol), H_2Asc, and PVP and in situ SERS spectra of 2,6-DMPI collected from an aqueous suspension of 40 nm Ag nanocubes, 2,6-DMPI, H_2Asc, and PVP before and after the addition of 50 μL of Na_2PdCl_4 precursor at room temperature (21 °C).

DOI: 10.1021/jacs.8b04824
J. Am. Chem. Soc. 2018, 140, 8340−8349

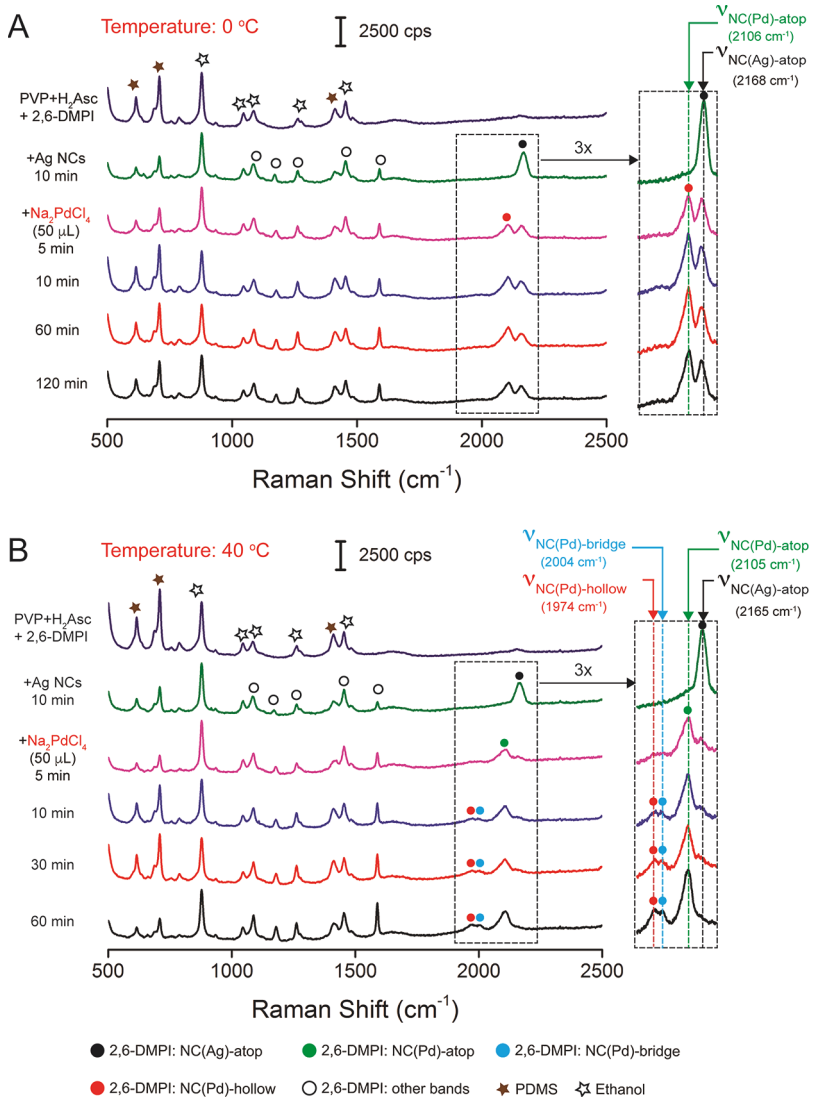

Figure 6. Raman spectrum recorded from an aqueous solution containing 2,6-DMPI (predissolved in ethanol), H_2Asc, and PVP and in situ SERS spectra of 2,6-DMPI collected from an aqueous suspension of 40 nm Ag nanocubes, 2,6-DMPI, H_2Asc, and PVP before and after the addition of 50 μL of Na_2PdCl_4 precursor at (A) 0 °C (ice bath) and (B) 40 °C (oil bath).

H_2Asc at room temperature should undergo a solution-phase reduction for the generation of Pd atoms,[35] followed by their initial deposition onto the edges of Ag nanocubes while surface diffusion could move some of the Pd adatoms onto the corners and side faces. At t = 5 min post the introduction of Na_2PdCl_4, we observed the $\nu_{NC(Pd)\text{-}atop}$ band at 2104 cm^{-1} (marked by green dot) while the $\nu_{NC(Ag)\text{-}atop}$ band was still positioned at 2162 cm^{-1} although its peak intensity had dropped. The ratio between the peak intensities of the $\nu_{NC(Pd)\text{-}atop}$ and $\nu_{NC(Ag)\text{-}atop}$ bands was 1.40:1. This result suggested that a small number of Pd atoms derived from the solution-phase reduction nucleated from the edges of the Ag nanocubes in the form of individual Pd adatoms, leading to the formation of a surface consisting of both Ag and Pd atoms, to which the 2,6-DMPI molecules would bind in the atop configuration.

As the reaction progressed to t = 10 min, the positions of all peaks in the spectra remained the same except that there was an increase in the intensity ratio between the $\nu_{NC(Ag)\text{-}atop}$ and $\nu_{NC(Pd)\text{-}atop}$ bands to 2.32:1. At t = 30 min, the $\nu_{NC(Ag)\text{-}atop}$ band became a shoulder peak while the $\nu_{NC(Pd)\text{-}atop}$ band gained dominance. In addition, we observed two new weak peaks (still relatively weak) at 2007 and 1973 cm^{-1}, which could be assigned to $\nu_{NC(Pd)\text{-}bridge}$ and $\nu_{NC(Pd)\text{-}hollow}$, respectively. By t = 60 min, the $\nu_{NC(Pd)\text{-}bridge}$ and $\nu_{NC(Pd)\text{-}hollow}$ bands became well-identified as the $\nu_{NC(Pd)\text{-}atop}$ peak remained essentially unchanged. The appearance of $\nu_{NC(Pd)\text{-}bridge}$ and $\nu_{NC(Pd)\text{-}hollow}$ bands indicated that, as more and more Pd was deposited on the edges of the Ag nanocube, the Pd adatoms started to evolve into monolayer and then multilayers on the edges of a nanocube, followed by surface diffusion to the corners and side faces. As shown in Figure 2B, the hollow configuration is only allowed for Pd atoms deposited on the {111} facets at the corner sites as constrained by the atomic arrangement. As for the bridge configuration, it is allowed for Pd adatoms deposited on both the {110} and {100} facets, corresponding to the edges and side faces. The observation of $\nu_{NC(Pd)\text{-}atop}$ peak suggested that some of the Pd atoms could still be deposited on the surface as individual atoms.

We further used ICP-MS to analyze the sample obtained at the reaction time of 60 min. Our results indicate that 42.3% of the added Na_2PdCl_4 was converted to Pd atoms, followed by their deposition onto the Ag nanocubes (Table S5). In

DOI: 10.1021/jacs.8b04824
J. Am. Chem. Soc. 2018, 140, 8340−8349

comparison with the conversion rate of 46.6% for Na_2PdCl_4 when 2,6-DMPI was not involved in the reaction solution (see Table S1), we argued that the SERS probe did not interfere with the reduction of Na_2PdCl_4. We further used TEM to characterize the sample. Figure S5A indicates that the morphology of the nanoparticles was essentially the same as those shown in Figure 3A where no 2,6-DMPI was added into the reaction solution. When the injection volume was increased to 600 μL in the presence of 2,6-DMPI, Figure S5B, C shows the transformation of nanocubes into nanoframes after the removal of Ag with an aqueous mixture of $Fe(NO_3)_3$ and HNO_3, in agreement with the results shown in Figure 3C, D. Taken together, we believed that the presence of 2,6-DMPI molecules in the reaction solution did not alter the reduction pathway of Na_2PdCl_4, nor the deposition of the resultant Pd atoms, which still preferred heterogeneous nucleation from the edges of the Ag nanocubes.

We also conducted another control experiment by following the same in situ protocol except that no H_2Asc was added. As shown in Figure S6, after 10 min post the addition of Ag nanocubes, we observed the peak of $\nu_{NC(Ag)\text{-}atop}$ at 2179 cm^{-1} in the SERS spectrum, indicating the adsorption of 2,6-DMPI onto the surface of the Ag nanocubes. However, when aqueous Na_2PdCl_4 was introduced, we did not resolve any peaks associated with the $\nu_{NC(Pd)\text{-}atop}$, $\nu_{NC(Pd)\text{-}bridge}$, and $\nu_{NC(Pd)\text{-}hollow}$ bands up to t = 60 min. The $\nu_{NC(Ag)\text{-}atop}$ band also became too weak to be identified. These results are completely different from those SERS spectra shown in Figure 5 when H_2Asc was involved in the synthesis. In the absence of H_2Asc, we argue that the galvanic replacement reaction would dominate. Some of the resultant Pd atoms will be deposited on the side faces of the Ag nanocubes, reducing the number of Pd atoms deposited on the edges where hot spots are located and thus making it difficult to detect the Pd atoms by SERS. Additionally, any dissolution of Ag from the sharp edges or corners of the nanocubes would deteriorate the SERS activity. Taken together, we believe that this in situ method also has the capability to distinguish the deposition of Pd on Ag nanocubes via galvanic replacement versus chemical reduction.

It should be pointed out that we performed in situ SERS measurements by withdrawing aliquots of 25 μL from the reaction solution under stirring at different reaction time points, followed by addition of the sample into a PDMS cell, optimization of optics and the spectrometer, and collection of a Raman spectrum in the *extended* mode (see details in the Experimental Section). Typically, it took 1−2 min to get the sample ready for spectral collection, together with another 2 min to complete the collection. The entire process took about 4 min from the withdrawal of sample to the completion of spectral recording. The time point marked in Figure 5 corresponds to the moment at which the collection of spectrum was initiated, relative to t = 0 min when the Na_2PdCl_4 precursor was introduced. To capture the heterogeneous nucleation events within a period of time shorter than 5 min, we revised our standard procedure by collecting the time-dependent SERS spectra in the *static* mode (see details in the Experimental Section). Figure S7 shows a series of Raman/SERS spectra obtained by withdrawing one sample from the reaction solution at t = 50 s after the addition of Na_2PdCl_4, and then subjecting it to Raman measurements from t = 1.5 min for another four scans up to t = 5.5 min. The spectra indicate that the ratio between the peak intensities of the $\nu_{NC(Pd)\text{-}atop}$ and $\nu_{NC(Ag)\text{-}atop}$ bands was increased from 0.15 to 1.49 as the time point was increased t = 1.5 to t = 5.5 min, confirming that the deposition of Pd atoms occurred rapidly on the edges of the Ag nanocubes in the form of individual Pd adatoms. As a result, a surface was created, to which the 2,6-DMPI molecules could bind to the Ag and Pd atoms in the atop configuration.

3.5. Investigating the Role of Temperature in Controlling the Heterogeneous Nucleation of Pd on Ag Nanocubes. The in situ SERS method opens an opportunity to investigate the role of reaction temperature in controlling the heterogeneous nucleation and growth of metal nanocrystals. Specifically, we conducted two sets of experiments by immersing the reaction container in an ice bath (at 0 °C) or oil bath (at 40 °C), respectively. Figure 6A shows the Raman/SERS spectra of the aliquots sampled from the reaction solution held at 0 °C. The Raman spectrum was essentially the same as what was collected when the synthesis was conducted at room temperature (21 °C, see Figure 5). After introducing the Ag nanocubes and waiting for 10 min, we observed the $\nu_{NC(Ag)\text{-}atop}$ peak at 2168 cm^{-1}, suggesting that the kinetics for the adsorption of 2,6-DMPI onto the surface of Ag nanocubes was comparable at 0 and 21 °C. At t = 5 min post the addition of Na_2PdCl_4, we observed both $\nu_{NC(Pd)\text{-}atop}$ and $\nu_{NC(Ag)\text{-}atop}$ bands appeared at 2106 and 2168 cm^{-1}, respectively, and ratio of their peak intensities was 1.07:1. As the reaction progressed to 10 min, the SERS spectrum only showed a slight increase in peak intensity ratio for the $\nu_{NC(Pd)\text{-}atop}$ and $\nu_{NC(Ag)\text{-}atop}$ bands to 1.34:1. It was difficult to resolve the $\nu_{NC(Pd)\text{-}bridge}$ and $\nu_{NC(Pd)\text{-}hollow}$ bands. The SERS spectra showed very little changes when the reaction time was prolonged from 10 to 120 min. This observation is completely different from the SERS data shown in Figure 5 for the synthesis conducted at 21 °C. Specifically, the reduction of Na_2PdCl_4 and thus the deposition of Pd became much slower at a lower temperature, as indicated by the smaller ratio between the peak intensities of $\nu_{NC(Pd)\text{-}atop}$ and $\nu_{NC(Ag)\text{-}atop}$ bands.

In comparison, Figure 6B shows the Raman/SERS spectra collected from the reaction solution for the synthesis conducted at 40 °C. Although the Raman spectrum and the SERS spectrum of the Ag nanocubes are similar to those shown in Figures 6A, the evolution of the SERS spectra was completely different after the introduction of Na_2PdCl_4. At t = 5 min post the introduction of Na_2PdCl_4, we observed the $\nu_{NC(Pd)\text{-}atop}$ peak at 2105 cm^{-1} but could barely detect the $\nu_{NC(Ag)\text{-}atop}$ peak. This result indicated great acceleration for both the reduction of Na_2PdCl_4 and deposition of Pd when the reaction temperature was raised to 40 °C. At t = 10 min, we could easily resolve $\nu_{NC(Pd)\text{-}bridge}$ and $\nu_{NC(Pd)\text{-}hollow}$ peaks at 2004 and 1974 cm^{-1}, respectively. As the reaction progressed from 10 to 60 min, both $\nu_{NC(Pd)\text{-}bridge}$ and $\nu_{NC(Pd)\text{-}hollow}$ peaks showed major increases in intensity.

Collectively, we believe that the in situ SERS spectra at different temperatures provide a clear picture about the reduction, deposition, and surface diffusion processes involved in the nucleation and early stage deposition of Pd on Ag nanocubes. At 0 °C, both the reduction and deposition kinetics would be retarded while the diffusion process was largely suppressed. In this case, only a small portion of the added Na_2PdCl_4 was reduced for the deposition of Pd as individual adatoms on the Ag surface, resulting in the presence of both Pd and Ag atoms on the outermost surface for binding with 2,6-DMPI in the atop configuration. Because the diffusion of Pd adatoms across the Ag surface was largely suppressed, the

DOI: 10.1021/jacs.8b04824
J. Am. Chem. Soc. 2018, 140, 8340−8349

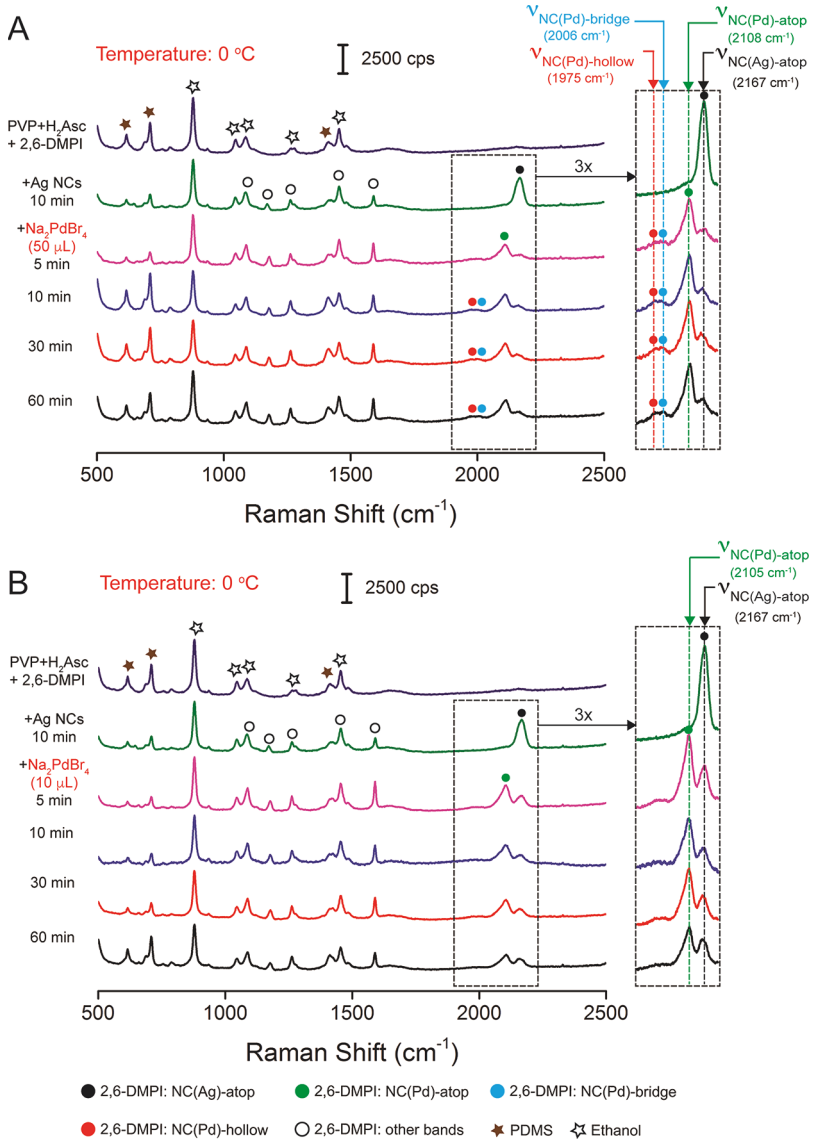

Figure 7. Raman spectrum recorded from an aqueous solution containing 2,6-DMPI (predissolved in ethanol), H_2Asc, and PVP, and time-dependent SERS spectra of 2,6-DMPI collected from an aqueous suspension of 40 nm Ag nanocubes, 2,6-DMPI, H_2Asc, and PVP before and after the addition of (A) 50 μL and (B) 10 μL of aqueous Na_2PdBr_4 held at 0 °C with an ice bath.

SERS spectrum was essentially the same as what was observed at t = 5 min when the reaction time was prolonged. At 40 °C, it is anticipated that the increase in temperature could greatly accelerate the reduction, deposition, and surface diffusion processes. Even at t = 5 min, a significant portion of the Na_2PdCl_4 precursor could be reduced to generate Pd atoms for their deposition on the edges of the Ag nanocubes to create a monolayer of Pd adatoms on Ag, leading to the dominance of $\nu_{NC(Pd)\text{-atop}}$ peak in the absence of $\nu_{NC(Ag)\text{-atop}}$ in the SERS spectrum. As the reaction progressed, more Pd atoms would be deposited on the edges of the Ag nanocubes, and ultimately, more Pd adatoms were able to migrate via surface diffusion to the corners and side faces, giving rise of both $\nu_{NC(Pd)\text{-bridge}}$ and $\nu_{NC(Pd)\text{-hollow}}$ peaks. Nevertheless, the $\nu_{NC(Pd)\text{-atop}}$ peak remained in the SERS spectrum because some of the Pd atoms could still exist on the surface as individual atoms.

It should be acknowledged that the in situ SERS spectra shown in Figure 6 were highly reproducible in terms of peak position and intensity as long as the same batch of Ag nanocubes was used. To further evaluate the stability of SERS signal intensity, we performed another set of experiments to collect time-elapsed SERS spectra in the *static* mode (see the Experimental Section). Because there was very little change to the SERS spectra at 0 °C after t = 5 min due to the very slow reduction kinetics of the Pd(II) precursor (see Figure 6A), we collected another set of in situ SERS spectra by keeping the reaction conditions unaltered but changing the Raman collection mode. At t = 5 min post the introduction of Na_2PdCl_4, we started to record SERS spectra using the *static* mode. As shown in Figure S8, the SERS signals were rather stable up to a duration of 10 s at a collection time of 1 s. On the basis of the 10 data points of peak intensity for the $\nu_{NC(Pd)\text{-atop}}$ band, we estimated a fluctuation of ~17% in SERS signal over a period of 10 s. Taken together, we believe that this in situ SERS technique embraces a great potential to extract reliable data for kinetic analysis.

3.6. Examining the Role of Pd(II) Precursor in Affecting the Deposition of Pd on Ag Nanocubes. To further demonstrate the unique capacity of this in situ method in revealing the mechanistic details behind the deposition of

DOI: 10.1021/jacs.8b04824
J. Am. Chem. Soc. 2018, 140, 8340−8349

Pd on Ag nanocubes, we replaced the Na_2PdCl_4 precursor with Na_2PdBr_4 while keeping all other parameters unaltered. Most recently, Xia and co-workers demonstrated that the reduction of Na_2PdBr_4 by H_2Asc would take a surface pathway at 0 °C.[35] In this case, the precursor ions would initially adsorb onto the surface of a nanocrystal, followed by their reduction to atoms. Figure 7A shows a set of Raman/SERS spectra collected from the reaction solution of a synthesis conducted in an ice bath (0 °C) when 50 μL of aqueous Na_2PdBr_4 was introduced. The Raman spectrum and the SERS spectrum of the Ag nanocubes were essentially the same as those shown Figure 6A. At t = 5 min post the introduction of Na_2PdBr_4 solution, we observed a strong $\nu_{NC(Pd)\text{-atop}}$ peak and a weak $\nu_{NC(Ag)\text{-atop}}$ peak, together with two weak peaks of $\nu_{NC(Pd)\text{-bridge}}$ and $\nu_{NC(Pd)\text{-hollow}}$ in the spectrum. This result is similar to the spectrum at t = 5 min in Figure 6B when Na_2PdCl_4 was used as a precursor at 40 °C, but it is completely different from what is shown in Figure 6A at t = 5 min and at 0 °C. From 10 to 60 min, the SERS spectra show little change except that both the $\nu_{NC(Pd)\text{-bridge}}$ and $\nu_{NC(Pd)\text{-hollow}}$ bands at 2006 and 1975 cm^{-1} became more dominant.

According to the surface reduction mechanism, we argued that the $PdBr_4^{2-}$ ions would first adsorb onto the {110}, {111}, and {100} facets on the Ag nanocubes via collisions, followed by a surface reduction pathway to generate Pd atoms by H_2Asc. Because the adsorption of $PdBr_4^{2-}$ ions could still occur at 0 °C, a large number of Pd atoms were generated at t = 5 min, leading to a high coverage of Pd atoms across the surface of the Ag nanocubes. In this case, the $\nu_{NC(Ag)\text{-atop}}$ peak became very weak while $\nu_{NC(Pd)\text{-atop}}$, $\nu_{NC(Pd)\text{-bridge}}$, and $\nu_{NC(Pd)\text{-hollow}}$ bands all appeared in the SERS spectrum. To further support our argument, we performed another experiment with 10 μL of Na_2PdBr_4 solution while leaving other conditions unchanged. In this case, we hypothesize that fewer $PdBr_4^{2-}$ ions would adsorb onto the surface of the Ag nanocubes, leading to the generation of Pd as individual adatoms, with which 2,6-DMPI would bind in the atop configuration only. As shown in Figure 7B, after the injection of aqueous Na_2PdBr_4, we only observed the $\nu_{NC(Pd)\text{-atop}}$ and $\nu_{NC(Ag)\text{-atop}}$ peaks at 2105 and 2167 cm^{-1} with essentially no $\nu_{NC(Pd)\text{-bridge}}$ and $\nu_{NC(Pd)\text{-hollow}}$ in the period from 5−60 min. This observation supports the surface reduction mechanism.

We further evaluated the role of temperature in controlling the deposition of Pd on the Ag nanocubes using Na_2PdBr_4 as the Pd(II) precursor. Figure S9 shows a set of Raman/SERS spectra collected from the reaction solution of a synthesis conducted in an oil bath (40 °C) when 50 μL of aqueous Na_2PdBr_4 was introduced. At t = 5 min post the addition of Na_2PdBr_4 solution, we observed all the peaks for $\nu_{NC(Pd)\text{-atop}}$, $\nu_{NC(Pd)\text{-bridge}}$, and $\nu_{NC(Pd)\text{-hollow}}$. This result is similar to the spectrum at t = 5 min in Figure 7A when Na_2PdBr_4 was used as a precursor at 0 °C except that we could not identify the $\nu_{NC(Ag)\text{-atop}}$ peak. We expect that the surface diffusion of Pd adatoms would be accelerated at 40 °C, leading to a decrease for the Ag atoms on the surface of the Ag−Pd nanocubes. It is worth emphasizing that this observation is completely different from what is shown in Figure 6B at t = 5 min when 50 μL of Na_2PdCl_4 was involved in the reaction solution at 40 °C. In the latter case, we could only resolve the $\nu_{NC(Pd)\text{-atop}}$ peak, not the $\nu_{NC(Pd)\text{-bridge}}$ and $\nu_{NC(Pd)\text{-hollow}}$ peaks. From 10 to 60 min, the SERS spectra in Figure S8 remained essentially unchanged except that both the $\nu_{NC(Pd)\text{-bridge}}$ and $\nu_{NC(Pd)\text{-hollow}}$ bands became more predominant, consistent with those shown in Figure 7A at 0 °C. These results are consistent with a surface reduction mechanism at 40 °C.[35] Collectively, our in situ SERS results suggest that surface reduction could serve as an effective route to the deposition of Pd on Ag nanocubes.

4. CONCLUSIONS

In summary, we have demonstrated the use of 2,6-DMPI as a sensitive probe for in situ atomic-level tracking of the heterogeneous nucleation of Pd on Ag nanocubes by SERS. Because the isocyanide group binds to Ag and Pd via σ donation and π-back-donation, respectively, we can simply monitor the deposition of Pd on Ag nanocubes by following the distinctive stretching frequency of 2,6-DMPI, ν_{NC}, using SERS. More significantly, we discovered that the isocyanide group could bind to one, two, and three adjacent Pd atoms to generate the atop, bridge, and hollow binding configurations, respectively, to display different vibrational frequencies. This unique feature makes it possible to use 2,6-DMPI as a distinctive reporter for characterizing Pd atoms being deposited onto different types of facets on Ag nanocubes with different arrangements. By directly introducing 2,6-DMPI molecules into the reaction solution, we further demonstrated atomic-level dynamic tracking of heterogeneous nucleation of Pd on Ag nanocubes by monitoring the ν_{NC} bands through time-dependent SERS spectra. This in situ tracking method with atomic resolution allows us to investigate the roles played by reaction temperature and the type of Pd(II) precursor in affecting the heterogeneous nucleation and deposition of Pd on Ag nanocrystals. With further development, this technique will also support the rational synthesis of bimetallic nanocrystals involving other noble metals such as Ru, Rh, and Ir.

■ ASSOCIATED CONTENT

Supporting Information

The Supporting Information is available free of charge on the ACS Publications website at DOI: 10.1021/jacs.8b04824.

Graphic illustration of a Ag nanocube; ordinary Raman spectra, TEM images, in situ SERS spectra, and contents of Pd and Ag in the solid product and supernatant using ICP-MS analysis (Figures S1−S9, Tables S1−S5, and Appendices 1−3) (PDF)

■ AUTHOR INFORMATION

Corresponding Author

*dong.qin@mse.gatech.edu

ORCID

Dong Qin: 0000-0001-5206-5912

Notes

The authors declare no competing financial interest.

■ ACKNOWLEDGMENTS

We acknowledge the support from the National Science Foundation (CHE-1708300) and (CMMI-1634687), start-up funds from the Georgia Institute of Technology (GT), and a 3M nontenured faculty award. We also acknowledge the use of the characterization facility at the Institute of Electronics and Nanotechnology (IEN) at GT.

■ REFERENCES

(1) Woodruff, D. P.; Delchar, T. A. *Modern Techniques of Surface Science*, 2nd ed.; Cambridge University Press: Cambridge, U.K., 1994.

DOI: 10.1021/jacs.8b04824
J. Am. Chem. Soc. 2018, 140, 8340−8349

(2) Somorjai, G. A. *Introduction to Surface Chemistry and Catalysis*, 2nd ed.; John Wiley & Sons: New York, 2010.
(3) Tao, F.; Salmeron, M. *Science* **2011**, *331*, 171.
(4) Zaera, F. *Chem. Rev.* **2012**, *112*, 2920.
(5) Wu, J.; Shan, H.; Chen, W.; Gu, X.; Tao, P.; Song, C.; Shang, W.; Deng, T. *Adv. Mater.* **2016**, *28*, 9686.
(6) Gao, W.; Hood, Z. D.; Chi, M. *Acc. Chem. Res.* **2017**, *50*, 787.
(7) Jeanmaire, D. L.; Van Duyne, R. P. *J. Electroanal. Chem. Interfacial Electrochem.* **1977**, *84*, 1.
(8) Moskovits, M. *J. Chem. Phys.* **1978**, *69*, 4159.
(9) Zou, S.; Williams, C. T.; Chen, E. K.-Y.; Weaver, M. J. *J. Am. Chem. Soc.* **1998**, *120*, 3811.
(10) Joseph, V.; Engelbrekt, C.; Zhang, J.; Gernert, U.; Ulstrup, J.; Kneipp, J. *Angew. Chem., Int. Ed.* **2012**, *51*, 7592.
(11) Zhang, H.; Zhang, X.-G.; Wei, J.; Wang, C.; Chen, S.; Sun, H.-L.; Wang, Y.-H.; Chen, B.-H.; Yang, Z.-L.; Wu, D.-Y.; Li, J.-F.; Tian, Z.-Q. *J. Am. Chem. Soc.* **2017**, *139*, 10339.
(12) Xie, W.; Schlücker, S. *Chem. Commun.* **2018**, *54*, 2326.
(13) Joo, S. W.; Han, S. W.; Kim, K. *J. Colloid Interface Sci.* **2001**, *240*, 391.
(14) Suzuki, S.; Kaneko, S.; Fujii, S.; Marqués-González, S.; Nishino, T.; Kiguchi, M. *J. Phys. Chem. C* **2016**, *120*, 1038.
(15) Zhang, Q.; Blom, D. A.; Wang, H. *Chem. Mater.* **2014**, *26*, 5131.
(16) Zhao, L.; Chen, J.-L.; Zhang, M.; Wu, D.-Y.; Tian, Z.-Q. *J. Phys. Chem. C* **2015**, *119*, 4949.
(17) Gajdo, M.; Eichler, A.; Hafner, J. *J. Phys.: Condens. Matter* **2004**, *16*, 1141.
(18) Robertson, M. J.; Angelici, R. J. *Langmuir* **1994**, *10*, 1488.
(19) Kim, K.; Kim, K. L.; Choi, J.-Y.; Lee, H. B.; Shin, K. S. *J. Phys. Chem. C* **2010**, *114*, 3448.
(20) López-Tobar, E.; Hara, K.; Izquierdo-Lorenzo, I.; Sanchez-Cortes, S. *J. Phys. Chem. C* **2015**, *119*, 599.
(21) Gruenbaum, S. M.; Henney, M. H.; Kumar, S.; Zou, S. *J. Phys. Chem. B* **2006**, *110*, 4782.
(22) Hu, J.; Tanabe, M.; Sato, J.; Uosaki, K.; Ikeda, K. *J. Am. Chem. Soc.* **2014**, *136*, 10299.
(23) Hu, J.; Hoshi, N.; Uosaki, K.; Ikeda, K. *Nano Lett.* **2015**, *15*, 7982.
(24) Zhang, Y.; Liu, J.; Ahn, J.; Xiao, T.-H.; Li, Z.-Y.; Qin, D. *ACS Nano* **2017**, *11*, 5080.
(25) Bradshaw, A. M.; Hoffmann, F. M. *Surf. Sci.* **1978**, *72*, 513.
(26) Unterhalt, H.; Rupprechter, G.; Freund, H.-J. *J. Phys. Chem. B* **2002**, *106*, 356.
(27) Zeinalipour-Yazdi, C. D.; Willock, D. J.; Thomas, L.; Wilson, K.; Lee, A. F. *Surf. Sci.* **2016**, *646*, 210.
(28) Zhang, Q.; Li, W.; Wen, L.-P.; Chen, J.; Xia, Y. *Chem. - Eur. J.* **2010**, *16*, 10234.
(29) Li, J.; Liu, J.; Yang, Y.; Qin, D. *J. Am. Chem. Soc.* **2015**, *137*, 7039.
(30) Li, J.; Sun, X.; Qin, D. *ChemNanoMat* **2016**, *2*, 494.
(31) Li, J.; Wu, Y.; Sun, X.; Liu, J.; Winget, S. A.; Qin, D. *ChemNanoMat* **2016**, *2*, 786.
(32) Wu, Y.; Sun, X.; Yang, Y.; Li, J.; Zhang, Y.; Qin, D. *Acc. Chem. Res.* **2017**, *50*, 1774.
(33) Bae, S. C.; Lee, H.; Lin, Z.; Granick, S. *Langmuir* **2005**, *21*, 5685.
(34) Mammone, J.; Sharma, S.; Nicol, M. *J. Phys. Chem.* **1980**, *84*, 3130.
(35) Yang, T.-H.; Peng, H.-C.; Zhou, S.; Lee, C.-T.; Bao, S.; Lee, Y.-H.; Wu, J.-M.; Xia, Y. *Nano Lett.* **2017**, *17*, 334.

DOI: 10.1021/jacs.8b04824
J. Am. Chem. Soc. 2018, 140, 8340−8349